ICOLD Symposium on Sustainable Development of Dams and River Basins, 24th - 27th February, 2021, New Delhi

CASE STUDY OF ALPASLAN II DAM TWO-DIMENSIONAL DAM BREAK ANALYSIS

E. USTA
Hidro Dizayn Engineering Consultancy Construction and Trade Inc, Ankara, Turkey

ABSTRACT

Although dam break is not a common phenomenon, it could cause devastating and catastrophic consequences when it occurs. Estimation of downstream flood mapping due to dam break is a crucial point in order to determine potential risk areas and help preparation of emergency action plans. As a case study, dam break analysis of Alpaslan II Dam is carried out using remote sensing digital elevation data in order to assess dam break consequences preliminarily. Two-dimensional flow modelling tool of HEC-RAS software is used. Alpaslan II Dam and Hydropower Project (280 MW) is planned to be constructed on Murat River, which is one of the main branches of Euphrates River, at an approximate distance of 34 km to Muş city centre in the east of Turkey. This paper presents not only 2-dimensional unsteady flow modelling for dam break analysis of Alpaslan II Dam but also asses the effects of hydraulic variables on the analysis results. Firstly, optimum computational grid size is examined by running simulation from coarser grid to finer grid until convergency conditions on results are provided. Subsequently, the effects of different manning roughness coefficients and different breach parameters, which are obtained by the regression equations commonly used in literature, on inundation boundaries are examined. As a result of the analysis, preliminary flood mapping is visualized and potential inundated areas are determined with indicating the effects of hydraulic variables.

Keywords: *Dam Break, 2-Dimensional Flow Modelling, Flood Mapping, Inundation.*

1. INTRODUCTION

Dams have a significant role of countries' infrastructure both economically and socially. Purpose of the dams can be supplied potable or irrigation water, generated energy, provided flood control or used for recreation benefits. Despite the fact that there are many beneficial uses of the dams, they also feature risks due to their potential to fail. Although dam break is not a common phenomenon, it could cause devastating and catastrophic consequences when it occurs. In order to mitigate the impact of these consequences, risks should be analyzed regarding potential failure scenarios and essential precautions should be taken (Wahl, 1998).

As a first preliminary precaution, estimation of downstream flood mapping due to the dam break is specified in order to determine potential risk areas and help preparation of emergency action plans. This can be done utilizing hydraulic simulations. Simulations of dam break events have been increasingly used recently. The main objectives of the simulations are prediction of the outflow hydrograph and the routing of outflow hydrograph through the downstream in order to determine dam break consequences. Results of these simulations are inundation boundaries, outflow hydrographs, arrival time of flood waves and etc. Development of effective emergency action plans is directly related to the accurate prediction of these characteristics at a given location (Wahl, 2010).

There are many mechanisms that can be driving force of a dam failure such as overtopping due to extreme flood event, piping or seepage that can be observed as internal or underneath the dam, earthquake, landslide, equipment malfunction, structural damage and foundation failure (USACE, 2014). According to reports by the International Commission on Large Dams (ICOLD, 1973) and the United States Committee on Large Dams in cooperation with the American Society of Civil Engineers (ASCE/USCOLD, 1975), about 38% of all dam failures are caused by overtopping of the dam due to inadequate spillway capacity and by spillways being washed out during large inflows to the reservoir from heavy precipitation runoff. About 33% of dam failures are caused by seepage or piping through the dam or along internal conduits, while about 23% of the failures are associated with foundation problems, and the remaining failures are due to slope embankment slides, damage or liquefaction of earthen dams from earthquakes, and overtopping of the dam by landslide-generated waves within the reservoir.

In this study, preliminary assessments of dam break consequences are investigated using the relatively undetailed topographic data obtained from remote sensing. Overtopping failure mechanism is carried out for Alpaslan II Dam regarding that spillway is malfunctioned as dam failure scenario. The dam break analysis of Alpaslan II Dam is applied

using two-dimensional (2-d) flow modelling of HEC-RAS software developed by U.S Army Corps of Engineers. This paper presents not only 2-d unsteady flow modelling for the dam break analysis of Alpaslan II Dam but also asses the effects of hydraulic variables on the analysis results.

Firstly, the optimum computational grid size which affects the simulation time and results directly is investigated. Furthermore, the effects of different manning roughness coefficients and different breach parameters, which are obtained by the regression equations commonly used in literature, on inundation boundaries are examined. After the post-processing, flood mapping is visualized and potential inundated areas are determined with indicating the effects of hydraulic variables.

1.1 Study Area

Alpaslan II Dam and Hydroelectric Power Plant Project is located in the Eastern Anatolian Region of Turkey, within the provincial borders of Muş, on the Murat River, which is one of the main branches of the Euphrates River, at an approximate distance of 34 km to Muş city centre. Location of project area in Turkey is shown in Figure 1. Total catchment area of Murat River at Alpaslan II Dam axis is 17,500 km².

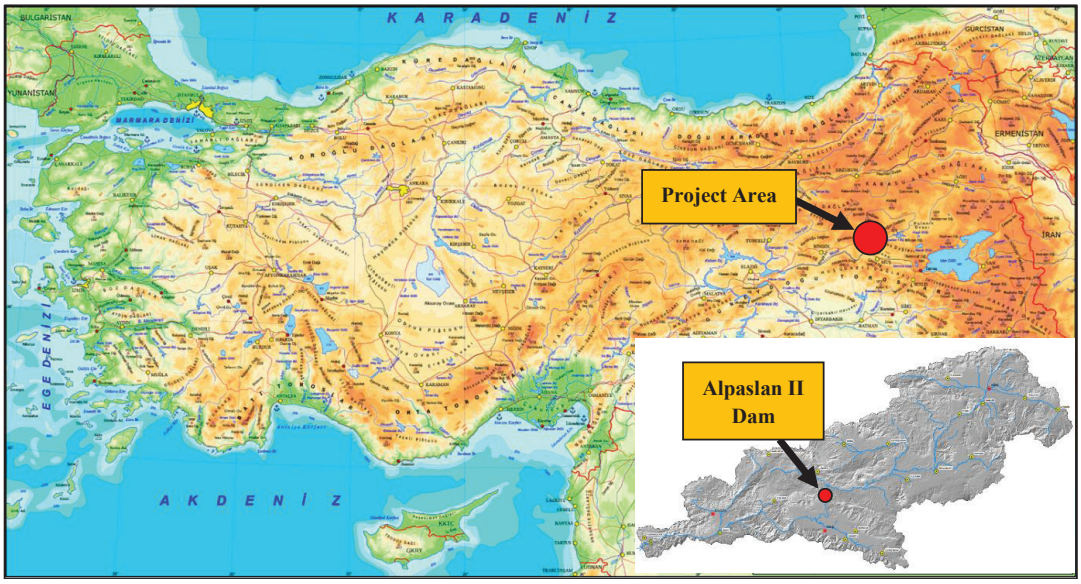

Figure 1 : Location of project area in Turkey

Alpaslan II Dam and Hydroelectric scheme is planned to utilize hydropower potential of Murat River between the elevations of 1368 masl and 1270 masl. With its 280-MW installed capacity at nominal head, the annual energy generation is expected to be approximately 832 GWh. The annual energy generation is expected to drop down to about 698 GWh when all projects at the upstream of Alpaslan II Dam is constructed and the fully development of the water resources in Murat River subbasin is completed. Three-dimensional (3-d) view of Alpaslan II Dam from downstream is given in Figure 2.

Figure 2 : 3-d view of Alpaslan II Dam from downstream

An asphalt core sand-gravel-rock fill dam embankment type is proposed for Alpaslan II Dam. The crest elevation of the embankment is set at 1371 masl, which results a height of 99 m from the thalweg. The storage at maximum operation level of Alpaslan II Dam is approximately 2.1 billion m³. Moreover, main characteristics of Alpaslan II Dam are summarized in Table 1.

Table 1 : Main Characteristics of Alpaslan II Dam

Parameters	**Alpaslan II Dam**
Thalweg Elevation	1272 masl
Crest Elevation	1371 masl
Height from Thalweg	99 m
Crest Width	10 m
Crest Length	829 m
Volume of Dam Body	8.8 hm³
Slope of U/S Dam Face (H:V)	1.8:1
Slope of D/S Dam Face(H:V)	1.6:1
Maximum Operation Level	1368 masl
Storage at Maximum Operation Level	2097 hm³
Storage at Crest Level	2237 hm³

2. MATERIALS AND METHOD

2.1 Hydraulic Model

Dam break is a phenomenon that the hydraulic characteristics of flow are variable with respect to time so full unsteady flow routing is more accurate for dam break analysis. Therefore, 2-d hydraulic model HEC-RAS (Version 5.0.5) is used to model the breach condition and to assess the complex flow conditions that exist at the downstream of Alpaslan II Dam using flow routing. The program solves either the 2-d Saint Venant equations or the 2-d Diffusion Wave equations.

Assuming that the flow is incompressible, 2-d full dynamic shallow water equations that govern the propagation of flood over complex natural topography form a system of three nonlinear partial differential equations as shown below (Altınakar et al. 2018). Equation 1 is the conservation of mass while Equation 2 and 3 are conservation of momentum in the horizontal plane.

$$\frac{\partial h}{\partial t}+\frac{\partial hu}{\partial x}+\frac{\partial hv}{\partial y}=q_v \tag{1}$$

$$\frac{\partial hu}{\partial t}+\frac{\partial h(uu+\frac{gh^2}{2})}{\partial x}+\frac{\partial hvu}{\partial y}=-ghS_{fx}-gh\frac{\partial z_b}{\partial x} \tag{2}$$

$$\frac{\partial hv}{\partial t}+\frac{\partial h(vv+\frac{gh^2}{2})}{\partial y}+\frac{\partial huv}{\partial x}=-ghS_{fy}-gh\frac{\partial z_b}{\partial y} \tag{3}$$

where t is time, h is flow depth, u and v are velocity components in x and y direction respectively, q_v is a source/sink flux term, g is gravitational acceleration, z_b is bed elevation with respect to datum, S_{fx} and S_{fy} are friction slope in x and y direction respectively. S_{fx} and S_{fy} are expressed using manning roughness coefficient, n as shown in Equation 4.

$$S_{fx}=\frac{un^2\sqrt{u^2+v^2}}{h^{4/3}} \quad \text{and} \quad S_{fx}=\frac{un^2\sqrt{u^2+v^2}}{h^{4/3}} \tag{4}$$

The system of three nonlinear partial differential equations can be written in vector form as given in Equation 5.

$$\frac{\partial \tilde{U}}{\partial t}+\frac{\partial \tilde{F}(\tilde{U})}{\partial x}+\frac{\partial \tilde{G}(\tilde{U})}{\partial y}=\tilde{S}(\tilde{U}) \tag{5}$$

The vector of conserved variables, U, the vectors of the fluxes in x and y directions, F(U) and G(U) respectively, and the vector of source terms due to friction and topography are given in Equation 6.

$$\tilde{U}=\begin{bmatrix}h\\hu\\hv\end{bmatrix}\ \tilde{F}(\tilde{U})=\begin{bmatrix}hu\\huu+\frac{gh^2}{2}\\huv\end{bmatrix}\ \tilde{G}(\tilde{U})=\begin{bmatrix}hv\\hvv+\frac{gh^2}{2}\\hvu\end{bmatrix}\ \tilde{S}(\tilde{U})=\begin{bmatrix}q_v\\-ghS_{fx}-gh\frac{\partial z_b}{\partial x}\\-ghS_{fy}-gh\frac{\partial z_b}{\partial y}\end{bmatrix} \tag{6}$$

2-d unsteady flow equations solver of HEC-RAS uses an Implicit Finite Volume algorithm that allows for larger computational time steps than explicit methods. The finite volume method provides an increment of improved stability and robustness over traditional finite difference and finite element techniques (USACE, 2016).

In order to select appropriate time step selection, variable time step based on Courant presented HEC-RAS as an option is used. The variable time step option can be used to improve model stability, as well as reduce computational time. This option provides a great flexibility in the analysis. According to User Manual of HEC-RAS, 2-d Diffusion Wave equations allow software to run faster and have greater stability properties so that 2-d Diffusion Wave equations are taken into account based on this information.

The inputs of the 2-d dam break hydraulic model include a digital terrain data of the study area, a user defined flow area for both reservoir and downstream valley, manning roughness coefficients, initial and boundary conditions and breach parameters.

The reservoir is modelled as a 2-d area without defining stage-storage relationship of Alpaslan II Dam hence, 2-d unsteady flow equations are solved for reservoir also such as downstream flow area. Although it is considered that the sediment condition in the reservoir may have some effects, presence of sediments is neglected in this study. The upstream boundary condition is defined as the inflow hydrograph, which consists of base flow, at the upstream end of reservoir within the defined area. On the other hand, the downstream boundary condition is defined as the normal depth corresponding to a value estimated with a friction slope of 0.001 which is approximately the bed slope of Murat River near the project site. Furthermore, as an initial condition, the water level in the reservoir is set to 1371 masl which is the crest elevation of Alpaslan II Dam. Therefore, it is assumed that overtopping failure occurs in first time step.

2.2 Digital Elevation Model

One of the most significant requirements of dam break analysis is the topographic data. The accuracy of topographic data shows the sensitivity of the analysis. In this study, digital elevation model (DEM) is created from ASTER-GDEM. This data is generally used in preliminary assessments. For detail studies, more accurate and precise topographic model which consists of ground survey data should be used.

ASTER GDEM topographic data set has a resolution of approximately 30 m. The ASTER GDEM obtained by USGS covers land surfaces between 83 N and 83 S and is comprised of 22 702 1 x 1 tiles. Tiles that contain at least 0.01% land area are included. The ASTER GDEM is distributed as Geo-referenced Tagged Image File Format (GeoTIFF) files and in geographic coordinates (latitude, longitude). The data are posted on 1 arc-second (approximately 30-m at the equator) grid and referenced to the 1984 World Geodetic System (WGS84)/1996 Earth Gravitational Model (EGM96) geoid (USGS, 2011). Digital elevation model of project obtained from ASTER-GDEM is given in Figure 3.

HEC-RAS uses gridded data for terrain modelling. A detailed elevation-volume curve is calculated for each of the cell to preserve all sub-grid terrain information. Detailed elevation versus area, wetted perimeter and roughness curves are developed for each face of each grid (USACE, 2016).

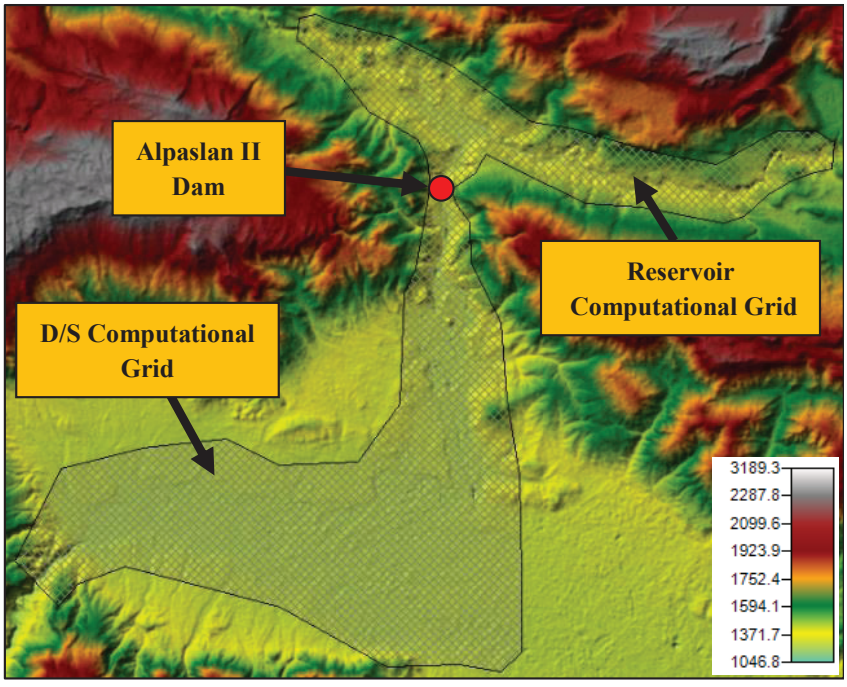

Figure 3 : Digital elevation model

2.3 Roughness

The roughness coefficient varies depending on such factors as grain size distribution of bed material, geometric properties of riverbeds and floodplain areas, the amount of vegetation cover and flow rate change (Unal & Bozkus, 2018). Although detail studies are required in order to determine roughness characteristics of project area, preliminary assessments do not generally consist of this. On the other hand, the effect of manning roughness coefficient on flood inundation boundaries is also examined. Constant coefficient such as n= 0.060 and n= 0.030 is assigned firstly and differences on results are compared. Furthermore, the cells are assigned manning roughness coefficients based on the classified land use data from the Corine Database (Coordination of information on the environment, 2012). Using classified land use map, the manning roughness values for project area are shown and listed in Figure 4.

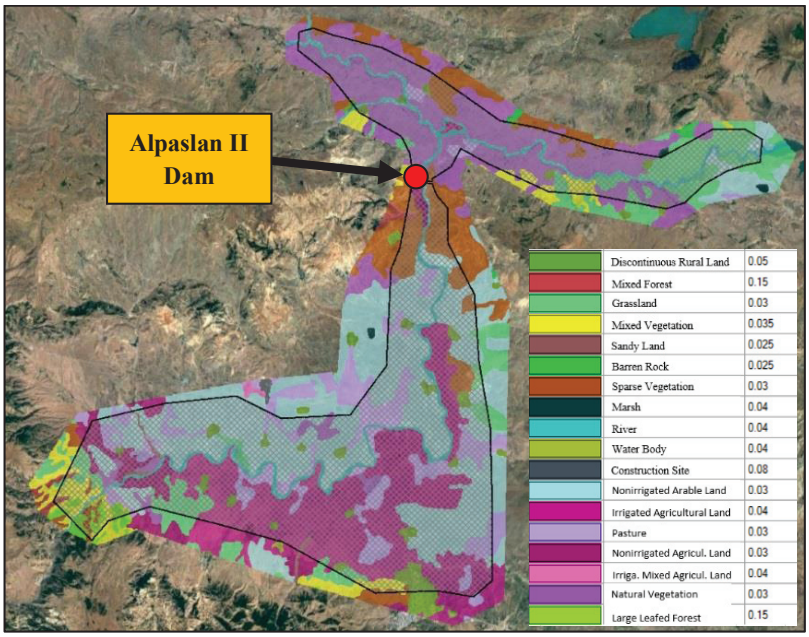

Figure 4 : Manning roughness coefficient in accordance with land cover

2.4 Breach Parameters

Trapezoidal shape is generally used in modelling the breach in dam break analysis (Froehlich, 2008). The estimation of dam breach location, dimensions, and development time are so important to assess the potential dam failure risk. The breach parameters directly affect the estimate of the outflow hydrograph coming out of the dam. However, it is a very hard process determining specifically these parameters in dam failure analysis. While the breach parameters are estimated, then 2-d unsteady flow modelling tool of HEC-RAS can be used to compute the outflow hydrograph from the breach and perform the downstream flow routing accordingly (USACE, 2014).

In this study, regression equations developed from historical dam failures in order to estimate breach characteristics and development time are used in accordance with overtopping failure mechanism for Alpaslan II Dam. Description of breach parameters is given in Figure 5.

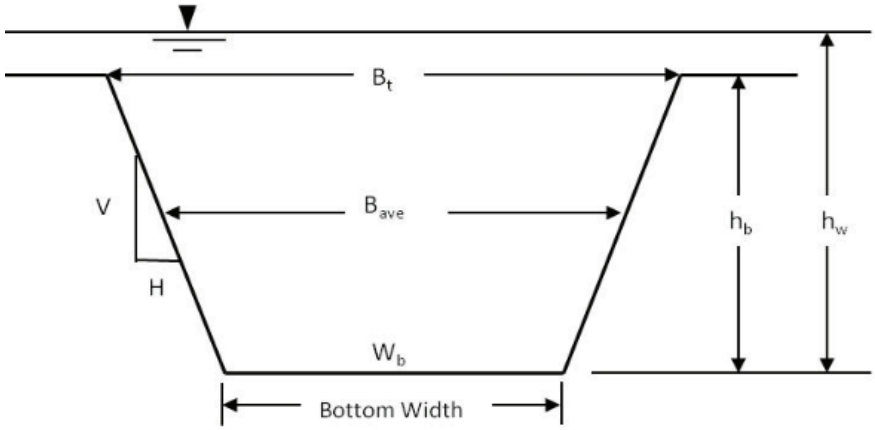

Figure 5 : Breach parameters (USACE, 2014)

The breach width is described as the average breach width (B_{ave}) in many equations, while HEC-RAS requires the breach bottom width (W_b) as input. The breach height (h_b) is the vertical extent from the top of the dam to the average

invert elevation of the breach. Many publications and equations also use the height of the water (h_w), which is the vertical extent from the maximum water surface to the invert elevation of the breach. The side slopes are expressed in H:V (USACE, 2014). Moreover, the other important parameter is breach formation time (t). It is the duration of time between the first breaching of the upstream face of the dam until the breach is fully formed.

Breach parameters using selected regression equations in literature are calculated and shown in Table 2 for overtopping failure mechanism.

Table 2 : Breach parameters of Alpaslan II Dam for overtopping failure mechanism

Method	W_b (m)	H:V	t (h)
Froelich (2008)	315	1	2.68
Von Thun Gillette (1990)	253	0.5	2.23
MacDonald et al (1984)	880	0.5	7.52
Froelich (1995)	455	1.4	3.67

3. RESULTS

Firstly, simulations are carried out from coarser computational grid to finer computational grid. Due to the fact that simulation time and quality of results are directly related to total number of computational cells, the most optimum size of computational cells is investigated. It is considered that the size of computational cells is appropriate where the solution is started to converge. Outflow peak values and inundation boundaries are compared in order to check solution convergency point. Outflow peak values from coarser grid to finer grid are presented in Table 3.

Dam break scenarios are simulated under different climatic initial conditions such as sunny day in dry season or rainy day during wet season. In this study, the base flow of Murat River in the analysis is roughly given as 1000 m³/s which can be seen as optimistic scenario and negligible in comparison with the scale of Alpaslan II Dam outflow hydrograph regarding its reservoir capacity of 2237 hm³ at crest level. Moreover, it is considered that Alpaslan II Dam spillway gates are closed or malfunctioned during the dam break event. Given the huge volume of water represented by Alpaslan II Dam outflow hydrograph, calculations could be started with a dry bed as a first approximation.

Table 3 : Outflow peak values

Cell Size (m)	Total Cells	Q_p (m³/s)	Simulation Time (h)
100 x 100	58,817	148,190	0.22
75 x 75	104,796	195,775	0.64
60 x 60	163,972	191,055	1.09
50 x 50	236,328	247,115	3.62
40 x 40	369,531	247,177	7.50
30 x 30	657,674	247,122	23.87

As shown in Table 3, outflow peak values converge to approximately 247,000 m³/s with the computational grid size of 50 m. In addition to this, flood inundation boundaries are compared for convergency. As shown in Figure 6, there is no significant difference in flood inundation boundary for different sizes of computational grid. Although there is a significant difference on peak value of outflow hydrographs for coarser computational grid size, there is no important difference on inundation boundaries. Thus, the grid size of 50 m is selected for other analysis and results. The outflow hydrograph and accumulated volume measured almost downstream of the dam as a result of dam break are given in Figure 7.

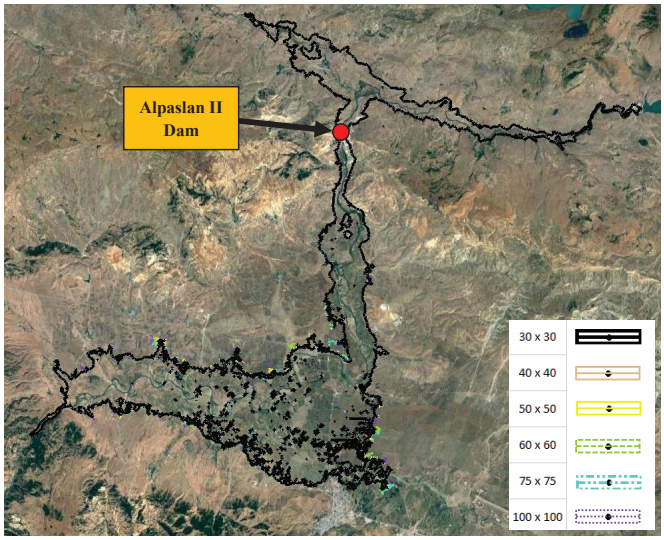

Figure 6 : Flood inundation boundaries with different grid size

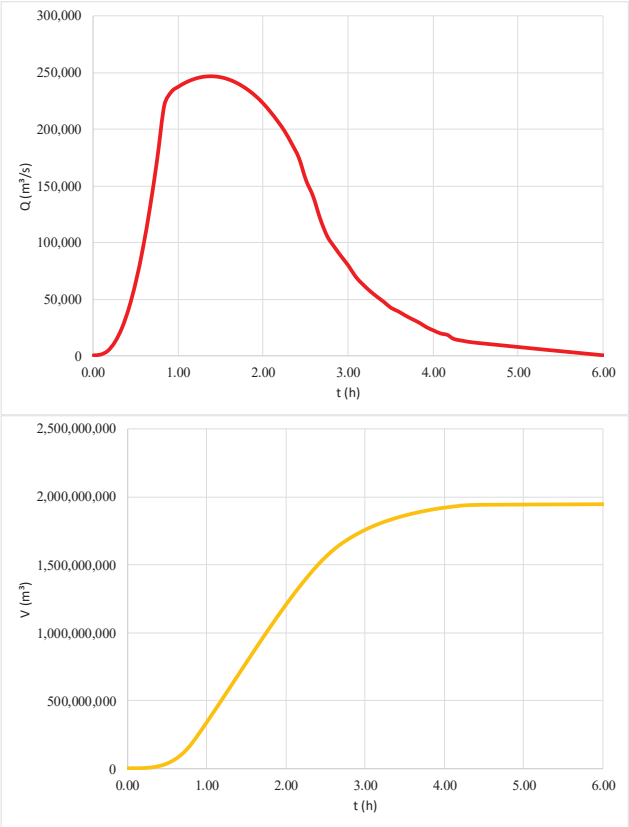

Figure 7 : Outflow Hydrograph and accumulated volume graphs measured almost downstream of the dam

Subsequently, the effect of manning roughness coefficients is examined. Flood inundation boundaries are compared to each other for constant manning roughness coefficient of 0.060, 0.030 and ones that assigned using land cover data. There are slight differences between flood inundation boundaries but no significant difference is observed as given in Figure 8.

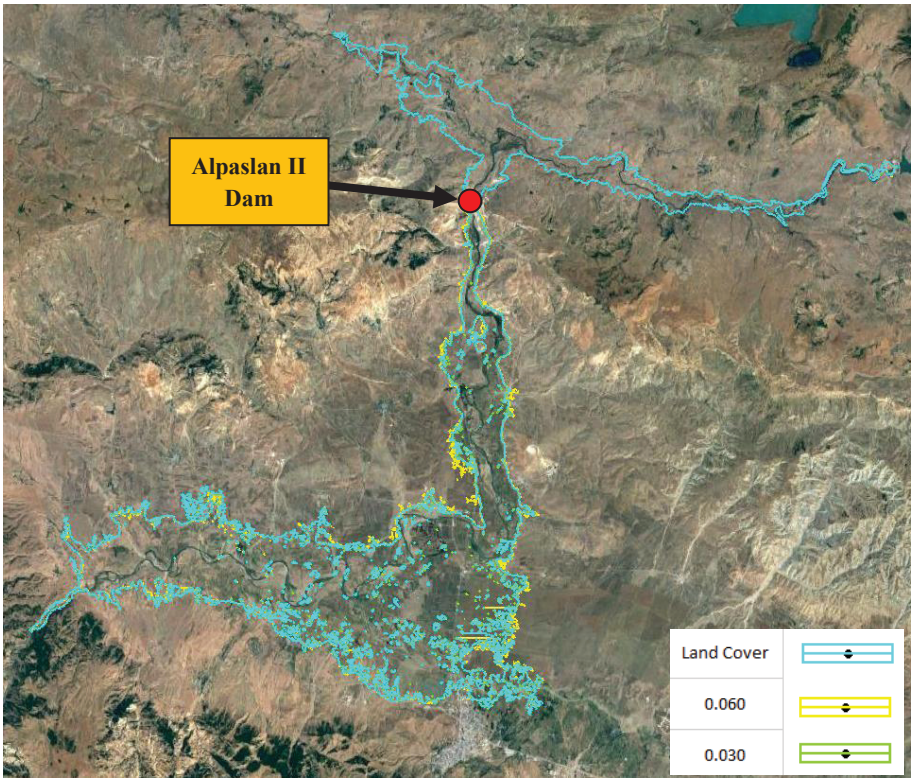

Figure 8 : Flood inundation boundaries with different manning roughness coefficient

Furthermore, the effect of different breach parameters on flood inundation boundaries are compared to each other in Figure 9. The regression equations which are used to calculate breach parameters are recommended by Froelich (2008), Von Thun Gillette (1990), MacDonald et al (1984) and Froelich (1995). For Von Thun Gillette equations, dam type is selected as dam with corewall with medium erodibility on the other hand, earth fill type is selected as non-homogenous or rockfill option for MacDonald et al (1984).

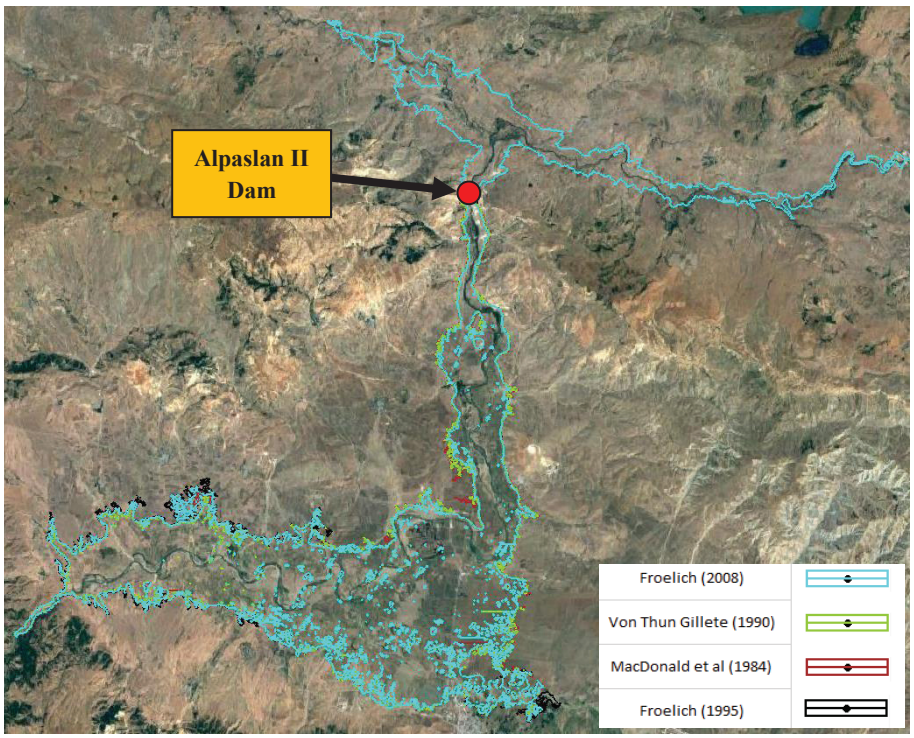

Figure 9 : Flood inundation boundaries with different regression equations

As shown Figure 9, the flood inundation boundary does not be significantly affected using different breach parameters.

As a result of this study, it is determined that there is no significant effect observed for different manning coefficients and breach parameters on inundation boundaries for this level of detail. Additionally, flood inundation boundary calculated using coarser computational grid has ignorable difference with ones that calculated using finer computational grid. However, the outflow hydrograph is significantly different for coarser computational grid.

Therefore, preliminary assessments of dam break analysis are carried out using relatively undetailed topographic data which has approximately 30 m resolution and potential risk areas are determined with 2-d flow modelling. Breach parameters are calculated using Froehlich (2008) equations. Manning roughness coefficient is assigned to project area in accordance with land cover data. As dam break scenario, the water level in the reservoir is set to 1371 masl which is the crest elevation of Alpaslan II Dam and it is assumed that overtopping failure occurs. According to this inputs, preliminary consequences of dam break analysis is presented in Figure 10.

The development time for the dam breach is 2.68 hours while the peak of the outflow from the dam occurs 1.42 hour after the beginning of the breaching process. The maximum flow rate from the dam is approximately 247,000 m^3/s. In addition to this, not only the peak value is important, but also the volume of flood hydrograph. According to Figure 10, although a great majority of Muş city centre is not affected significantly, the northern of Muş, some agricultural areas in Muş Plain and some villages are inundated due to dam break. The other important output of dam break analysis is flood arrival time. The length between location of Alpaslan II Dam axis and out of 2-dimensional flow area is 65 km. Flood arrival time is given in Figure 11. Flood wave reaches to downstream end of model at approximately 5 hours and it attenuates after this location with the effect of topography also. Furthermore, there is a potential high risk for residential areas in red line which shows the flood arrival time is shorter than 1.5 hours as shown in Figure 11.

4. DISCUSSIONS

Dam break is a phenomenon that is a complicated and comprehensive process and it is a very difficult issue to define the actual failure mechanism. However, using the increasing computational power, modelling techniques and literature studies, dam break modelling has been used in order to estimate potential risk areas.

In this study, the effects of the preliminary dam break analysis due to overtopping failure of Alpaslan II Dam is analyzed using 2-d unsteady flow modelling. Firstly, optimum computational grid size is examined. As a result of several simulations from coarser grid size to finer grid size, it is selected as 50 m due to the fact that the convergency condition are provided in this size. After that, the effects of different manning roughness coefficients which are assigned constantly

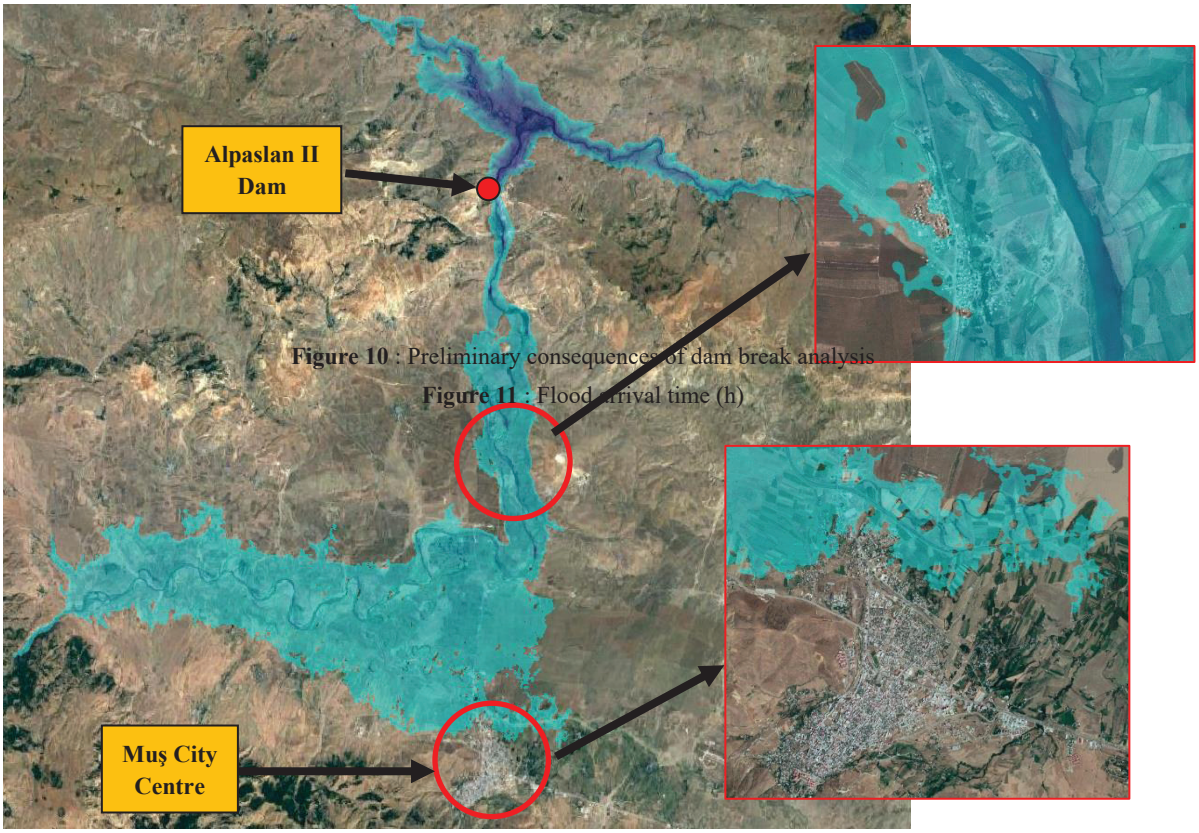

Figure 10 : Preliminary consequences of dam break analysis

Figure 11 : Flood arrival time (h)

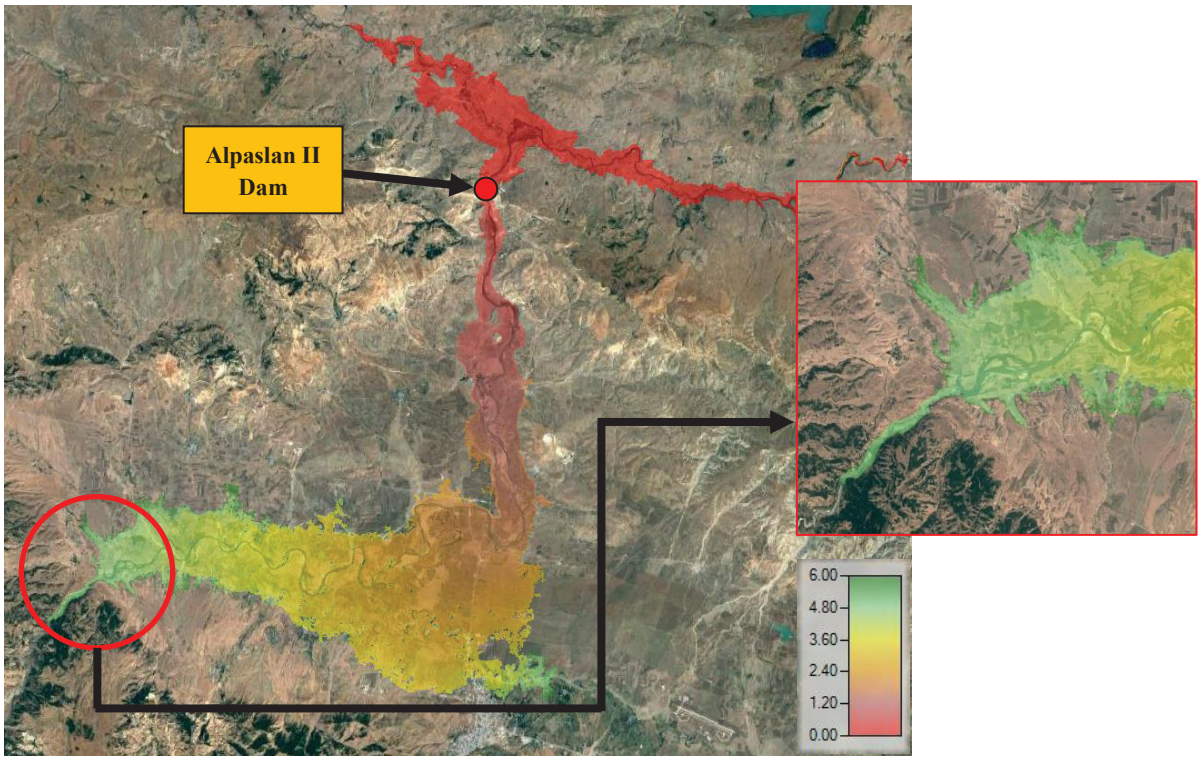

Figure 11 : Flood arrival time (h)

or variably and different breach parameters, which are calculated by different regression equations in literature, on flood inundation boundaries are investigated. There is no significant difference observed in flood inundation boundaries.

These simulations provide an initial idea of the potential risks due to the dam break event. After this preliminary assessment, detail assessments should be carried out. Additional simulations should be performed using more data and considering different scenarios. It is required that more precise maps comprised of ground survey data such as river

bathymetry, culverts, bridges, flood plain should be obtained in order to make more accurate analysis. It is considered that dam break analysis results and inundation area mapping will help decision makers to better understand the consequences and help the preparation of emergency action plans.

REFERENCES

Altinakar, M., McGrath, M., Ramalingam, V., Demby, J., Inci, G. 2018. Two-dimensional dam-break flood modeling and mapping for the USA. 5th *international symposium on dam safety., Istanbul, 27-31 October 2018*.

FEMA, 2013. Federal guidelines for inundation mapping of flood risks associated with dam incidents and failure. *First edition, FEMA p-946.*

Froehlich, D.C., 1995a. Peak Outflow from Breached Embankment Dam. *Journal of Water Resources Planning and Management, 121(1): 90-97*

Froehlich, D.C., 1995b. Embankment dam breach parameters revisited. *Proc., 1st Int. Conf. on Water Resources Engineering, American Society of Civil Engineers, New York, 887–891*

Froehlich, D.C., 2008. Embankment dam breach parameters and their uncertainties. *Journal of Hydraulic Engineering, 134(12): 1708-1721.*

Hidro Dizayn Engineering, Consultancy, Construction & Trade Inc., 2019. Alpaslan II Dam revised feasibility report. *Ankara, Turkey*

Hydrologic Engineering Center, 2014. HEC-RAS river analysis system, hydraulic reference manual. *CPD-69. U.S. Army Corps of Engineers, Hydrologic Engineering Center, 609 Second Street, Davis, CA.*

Hydrologic Engineering Center, 2014. Using HEC-RAS for dam break studies. *TD-39. U.S. Army Corps of Engineers, Hydrologic Engineering Center, 609 Second Street, Davis, CA.*

Hydrologic Engineering Center, 2016. HEC-RAS river analysis system, 2D modeling user' s manual. *CPD-68A. U.S. Army Corps of Engineers, Hydrologic Engineering Center, 609 Second Street, Davis, CA.*

MacDonald, T.C., Langridge-Monopolis, J., 1984. Breaching characteristics of dam failures. *Journal of Hydraulic Engineering, 110(5), 567-586*

Unal, I.C. & Bozkus, Z., 2018. Two-dimensional dam break analysis of Berdan Dam with HEC-RAS 5.0.3. 5th *international symposium on dam safety., Istanbul, 27-31 October 2018*.

Von Thun, J.L., Gillette, D.R., 1990. Guidance on breach parameters, unpublished internal document. *U.S. Bureau of Reclamation, Denver, Colorado, 17 p.*

Wahl, T.L. 1998. Prediction of embankment dam breach parameters – a literature review and needs assessment, DSO-98-004. *U.S. Department of the Interior Bureau of Reclamation Dam Safety Office.*

Wahl, T.L. 2010. Dam breach modeling – an overview of analysis methods. *Joint federal interagency conference on sedimentation and hydrologic modeling., Las Vegas, NV, 27 June -1 July 2010*.